

**COOLING RATE OF A TYPE I CHONDRULE FROM THE RENAZZO CR2 CHONDRITE INFERRED FROM Cu AND Ga DIFFUSION PROFILES IN METAL GRAINS.** N. Chaumard<sup>1</sup>, M. Humayun<sup>2</sup>, B. Zanda<sup>1</sup>, and R. H. Hewins<sup>1,3</sup>, <sup>1</sup>LMCM, MNHN, UMR 7202 – CNRS, 61 rue Buffon, 75005 Paris, France (nchaumard@mnhn.fr), <sup>2</sup>Department of Earth, Ocean, and Atmospheric Science & National High Magnetic Field Laboratory, Florida State University, 1800 E. Paul Dirac Drive, Tallahassee, FL 32310, USA, <sup>3</sup>Department of Earth and Planetary Sciences, Rutgers University, Piscataway, NJ 08854, USA.

**Introduction:** Chondrules are ubiquitous components of carbonaceous chondrites (CCs) [e.g. 1]. Different mechanisms have been proposed for chondrule formation [e.g. 2–9]. However, these mechanisms were suggested on the basis of cooling rates estimated for Type II (oxidized) chondrules, abundant only in ordinary chondrites, whereas CCs are dominated by Type I (reduced) chondrules. In order to provide new constraints on the heating mechanisms that prevailed throughout the protoplanetary disk in the early Solar System, we determined the cooling rates of a Type I chondrule in the Renazzo CR2 chondrite.

Since metal grains (Fe-Ni alloys) are abundant in association with chondrules [10], we used the method developed by [11] based on Cu and Ga zoning profiles measured by LA-ICP-MS in metal lumps attached to Type I chondrules. Volatile siderophile elements initially present in metal (e.g. Cu, Ga, and Ge) would be evaporated during a melting event then subsequently re-condensed at the exterior of metal grains [e.g. 12–14], and diffused inwards. Thus, analysis of Cu and Ga diffusion profiles can supply constraints on the high temperature event that formed Type I chondrules and their solid-state thermal history.

**Methods:** To avoid a possible under-estimation of cooling rates due to the random sectioning of metal grains, a fragment of Renazzo was imaged by CT scanning using a v|tome|x 240L from GE Sensing & Inspection Technologies Phoenix X|Ray in order to measure Cu and Ga diffusion profiles passing through the center of metal grains. Thus, we used X-ray tomography to locate Type I chondrules surrounded by large metal grains (Fig. 1). Then, we cut a fragment close to the equatorial planes of selected metal grains on Type I chondrules for further analyses. Finally, we polished our section until an equatorial plane of a metal grain corresponded to the polished surface of our sample.

SEM-BSE imaging and EDS analysis were obtained using a Tescan VEGA II LSU electron microscope. Laser ablation ICP-MS analyses were performed at Florida State University using a New Wave UP193 FX excimer laser ablation system coupled to a Thermo Element XR ICP-MS. Four diffusion profiles were measured through the centers of two metal grains (Fig. 1), using a 15  $\mu\text{m}$  spot size, 5  $\mu\text{m}\cdot\text{s}^{-1}$  speed, 50 Hz repetition rate, 100% power output (1.55  $\text{GW}\cdot\text{cm}^{-2}$ ).

Standards used were North Chile (Filomena) IIA iron meteorite, Hoba IVB iron meteorite, and NIST SRM 1263a steel. For a given element, each diffusion profile is characterized by a diffusion length-scale determined numerically.

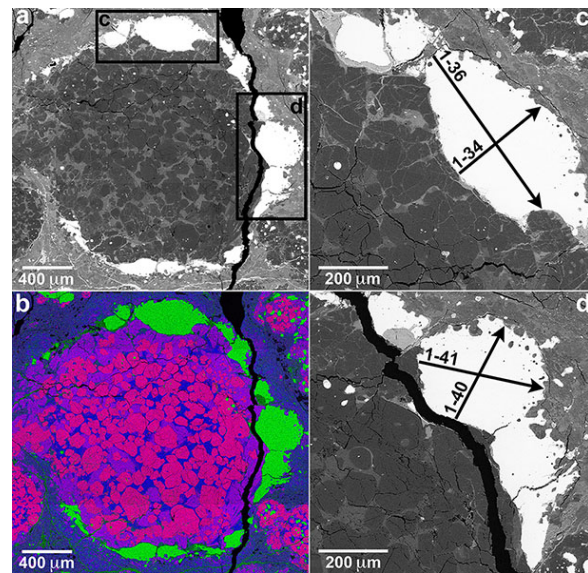


Figure 1: BSE image (a) and RGB compositional map (R=Mg G=Fe B=Si) (b) of the Type I chondrule from Renazzo analyzed in this study. (c) and (d) Higher magnification of the boxed regions in (a) showing laser tracks made by LA-ICP-MS.

**Results:** We observed chemical zonations for Cu and Ga in all profiles measured, also displaying practically ideal U-shaped profiles (Fig. 2). Diffusion length-scales vary between 35 and 120  $\mu\text{m}$  for profiles 1-41 and 1-36, respectively. Edges of metal grains are enriched in Cu and Ga, with maximal contents measured at  $\sim 140$  and  $\sim 12$  ppm, respectively, while cores are depleted in these volatile siderophile elements relative to the edges ( $\sim 0.20$  ppm Cu and  $\sim 0.05$  ppm Ga).

Since Cu diffuses more slowly than Ga at  $T > 1500$  K whereas it is the opposite at  $T < 1500$  K [15], we are able to provide an estimation of the temperature at which zoning profiles measured here were formed ( $T_p$ ) (Fig. 3). For all zoning profiles, ranges and means of  $T_p$  and cooling rates associated are reported in Tab. 1. Cooling rates are calculated from Cu diffusion profiles as  $\sim 4\text{--}65$   $\text{K}\cdot\text{h}^{-1}$  for peak temperatures of 1530–1630 K,

with an upper limit of  $\sim 0.1\text{--}520 \text{ K.h}^{-1}$  for a larger range of temperatures of 1273–1800 K (Fig 4).

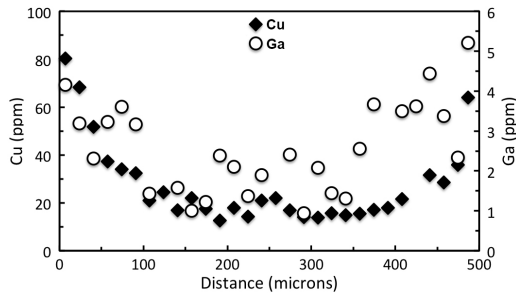


Figure 2: U-shaped zoning profile of Cu and Ga for the 1-36 laser track (see Fig. 1 for location).

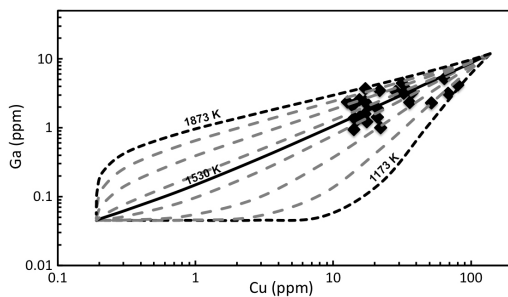


Figure 3: Ga vs. Cu for the diffusion profile 1-36 (diffusion length-scale = 120  $\mu\text{m}$ ), as a function of temperature from 1873 K to 1173 K in 100 K increments.

Profile	Diffusion length-scale (microns)	$T_p$ (K)		Cooling rate ( $\text{K.h}^{-1}$ )	
		Mean	Max. possible range	Mean	Max. possible range
1-34	55	1630	1473–1800	50	9–210
1-36	120	1530	1273–1800	4	0.1–45
1-40	80	1530	1373–1673	9	1–35
1-41	35	1573	1373–1800	65	6–520

Table 1: Diffusion length-scale,  $T_p$ , and cooling rates [8, Eq. (7)] calculated for each zoning profile measured in this work.

**Discussion:** The two metal grains analyzed for this Type I chondrule argue for a similar solid-state history. Cooling rates estimated here are similar to those calculated from six metal lumps in the Acfer 097 CR2 chondrites by [11],  $0.5\text{--}50 \text{ K.h}^{-1}$  for  $T_p \sim 1473 \text{ K}$  with a maximum possible range of  $0.1\text{--}400 \text{ K.h}^{-1}$  for  $T_p \sim 1200\text{--}1800 \text{ K}$ , and are close to those obtained from pyroxene exsolution in Type I chondrules from CCs [16, 17]. These results are consistent with cooling rates predicted by shock models proposed for chondrule formation ( $\sim 10\text{--}300 \text{ K.h}^{-1}$ , [e.g. 4]), and to a lesser extent by the X-wind model [e.g. 8] that seems only to be able to explain the lowest cooling rates ( $\sim <100 \text{ K.h}^{-1}$ ).

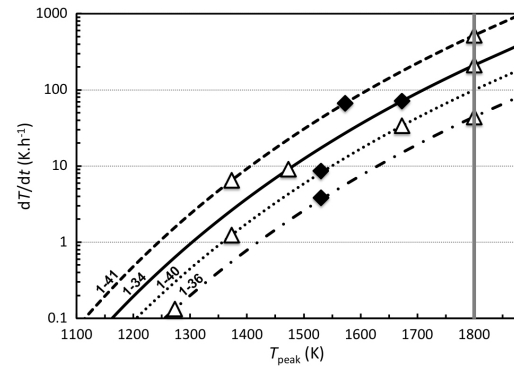


Figure 4: Cooling rates vs. peak temperatures calculated from the four diffusion profiles of Cu measured in this work (see Fig. 1 for location). Diffusion length-scale are 35  $\mu\text{m}$  for the 1-41 profile, 80  $\mu\text{m}$  for 1-40, 120  $\mu\text{m}$  for 1-36, and 55  $\mu\text{m}$  for 1-34. The melting point of Fe-Ni alloys is shown as the 1800 K line. Empty triangles indicate the upper and lower limit of the maximal possible range of  $T_p$  and cooling rates, while filled diamonds correspond to mean values of  $T_p$  and cooling rates for each diffusion profiles.

**Conclusion:** Cooling rates calculated here appear to be consistent with the predictions supplied by shock models and at variance with the higher cooling rates implied by a lightning model [e.g. 9]. Despite the fact that our quantitative results seem to indicate a similar solid-state thermal history for Type I chondrules in CCs, further systematic studies of cooling rates from metal and silicates could better constrain the high temperature event at the origin of chondrule formation.

**Acknowledgements:** We thank M. Garcia-Sanz for providing CT scans produced using the AST-RX computed tomography facility (UMS 2700 CNRS-MNHN, Paris). This study was supported by the ANR Program THEODULE.

**References:** [1] Zanda B. (2004) *EPSL*, 204, 1–7. [2] Hewins R. H. (1989) *Proc. NIPR Symp. Antarct. Meteorites*, 2, 202–222. [3] Desch S. J. and Connolly H. C. Jr. (2002) *MAPS*, 37, 183–207. [4] Morris M. A. and Desch S. J. (2010) *Astroph. J.*, 722, 1474–1494. [5] Libourel G. and Krot A. N. (2007) *EPSL*, 254, 1–8. [6] Asphaug E. et al. (2011) *LPS XLII*, Abstract #1647. [7] Joung M. K. R. et al. (2004) *Astroph. J.*, 606, 532–541. [8] Shu F. H. et al. (2001) *Astroph. J.*, 548, 1029–1050. [9] Pilipp W. et al. (1998) *Astron. & Astroph.*, 331, 121–146. [10] Weisberg M. K. et al. (1993) *GCA*, 57, 1567–1596. [11] Humayun M. (2012) *MAPS*, 47, 1191–1208. [12] Kong P. et al. (1999) *GCA*, 63, 3673–3682. [13] Zanda B. et al. (2002) *LPS XXXIII*, Abstract #1852. [14] Humayun M. et al. (2010) *LPS XLI*, Abstract #1840. [15] Righter K. et al. (2005) *GCA*, 69, 3145–3158. [16] Weinbruch S. and Müller W. F. (1995) *GCA*, 59, 3221–3230. [17] Cu villier P. et al. (2014) *This conference*.